Published in final edited form as:
ACS Chem Biol. 2013 April 19; 8(4): 840–848. doi:10.1021/cb400009f.

Small-molecule suppressors of *Candida albicans* biofilm formation synergistically enhance the antifungal activity of amphotericin B against clinical *Candida* isolates

Jianlan You[†,Δ], **Lin Du**[†,Δ], **Jarrod B. King**[†], **Brian E. Hall**[§], and **Robert H. Cichewicz**[*,†]
Natural Products Discovery Group, Institute for Natural Products Applications and Research Technologies, Stephenson Life Sciences Research Center, 101 Stephenson Parkway, University of Oklahoma, Norman, Oklahoma, 73019-5251, USA.EMD Millipore, 645 Elliott Avenue West, Suite 100, Seattle WA 98119, USA

Abstract

A new class of fungal biofilm inhibitors represented by shearinines D (**3**) and E (**4**) were obtained from a *Penicillium* sp. isolate. The inhibitory activities of **3** and **4** were characterized using a new imaging flow-cytometer technique, which enabled the rapid phenotypic analysis of *Candida albicans* cell types (budding yeast cells, germ tube cells, pseudohyphae, and hyphae) in biofilms populations. The results were confirmed by experimental data obtained from three-dimensional confocal laser scanning microscopy and 2,3- bis-(2-methoxy-4- nitro-5-sulfophenyl)-2*H*-tetrazolium-5-carboxanilide (XTT) assays. These data indicate that **3** and **4** inhibited *C. albicans* biofilm formation by blocking the outgrowth of hyphae at a relatively late stage of biofilm development (IC_{50} = 8.5 μM and 7.6 μM, respectively). However, **3** and **4** demonstrated comparatively weak activity at disrupting existing biofilms. Compounds **3** and **4** also exhibited synergistic activities with amphotericin B against *C. albicans* and others clinical *Candida* isolates by enhancing the potency of amphotericin B up to eight-fold against cells in both developing and established biofilms. These data suggest that the *Candida* biofilm disruption and amphotericin B potentiating effects of **3** and **4** could be mediated through multiple biological targets. The shearinines are good tools for testing the potential advantages of using adjunctive therapies in combination with antifungals.

Globally, *Candida* spp. are the most prevalent cause of mycoses[1–5] leading to an immense financial burden that exceeds ~$1 billion per year in the United States alone.[6] The majority of clinically-encountered *Candida* infections involve *Candida albicans*, which possesses an assortment of disease-promoting capabilities including the ability to form biofilms.[7–9] *Candida albicans* is remarkably versatile at establishing biofilms on a variety of surfaces ranging from human tissues (*e.g.*, mucosal membranes) to indwelling medical devices.[9–12] Biofilms shield *C. albicans* from attack by the immune system, as well as block antifungal antibiotics from reaching cells.[12–14] These defense-related attributes enable biofilms to function as infectious reservoirs,[9] which release new propagules both during and after treatment with antifungal therapeutics.

[*]To whom correspondence should be addressed. Tel: (405) 325-6969. rhcichewicz@ou.edu.
[†]Natural Products Discovery Group
[§]EMD Millipore
[Δ]These authors contributed equally to this work.

Supporting Information
Additional methods, natural products characterization, tables of NMR data, additional assay data for clinical isolate, and ITS sequence information for the fungal isolate (KS-017). This material is available free of charge via the Internet at http://pubs.acs.org.

JY, LD, JBK, and RHC declare no competing financial interest. BEH is an employee of EMD Millipore.

It has been observed that a subset of biofilm-embedded *C. albicans* cells exhibit a "persister" phenotype that is characterized by a state of extreme metabolic quiescence.[15–17] Persister cells are highly recalcitrant to the effects of antifungals agents,[18] and it is believed that they are a major contributing factor to infection relapse following the cessation of standard courses of antifungal antibiotics.[17] Persisters are genetically identical to drug-susceptible cells and it is likely that the biofilm environment provides the requisite context for enabling some *C. albicans* cells to stochastically enter into this semi-dormant state.[15]

For these reasons, biofilms are a clinically-relevant means with which *C. albicans* establishes persistent infections in humans.[12,19–22] It is anticipated that therapeutic interventions utilizing small-molecule inhibitors of biofilm formation would afford clinicians a valuable tool for reestablishing pharmacological control over recalcitrant *C. albicans* infections. However, pinpointing an appropriate chemical screening resource is a key step to identifying promising bioactive compounds that address this need.

Our research has focused on the rich chemical diversity of natural products for the discovery of bioactive small molecules that inhibit *C. albicans* biofilm formation. Although a handful of biofilm and morphological transition inhibitors have emerged in recent years,[23–26] many of these compounds suffer from mediocre potency or poor physiochemical characteristics. Natural products have long served as an unrivaled source of novel, drug-like molecules[27,28] and it is anticipated that our efforts will yield new inhibitors of *C. albicans* biofilm formation. Our earlier studies lend support to this approach with novel compounds including waikialoid A,[29] mutanobactin D,[30] and others[31] having been reported.

In this study, we report on the identification of a group of fungal-derived indole-alkaloids that inhibit *Candida* biofilm formation. Our study was greatly enhanced by the application of a new imaging flow-cytometer technique, which enabled us to readily quantify the morphological state distribution patterns of biofilm-associated *C. albicans* populations. We expect that this approach has the potential to provide tremendous insight into the biofilm formation process, as well as assist in the identification and classification of new biofilm inhibitors.

RESULTS AND DISCUSSION

Identification of *C. albicans* Biofilm Inhibitors

A soil sample collected in Ketchikan, Alaska, U.S.A. was received by our laboratory through an open-invitation sample-submission program. Isolate KS-017, which was determined to be a taxonomically undefined *Penicillium* sp. (based on ITS1-5.8S-ITS2 sequence homology – see Supporting Information). An ethyl acetate extract prepared from a small-scale culture of the fungus was found to inhibit *C. albicans* DAY185 biofilm formation (85% biofilm reduction at 100 μg mL^{-1}). Bioassay-guided fractionation yielded a single active fraction that was composed of several structurally-related compounds (based on comparisons of ^{1}H NMR data – data not shown). All of the major components in the sample were purified and characterized *via* nuclear magnetic resonance spectroscopy and mass spectrometry dereplication, as well as *de novo* structure determination. This afforded a new indole triterpenoid, 22,23-dehydro-shearinine A (**1**); two new indole diketopiperazines, 2-dehydroxy-3-demethoxy-okaramine B (**6**) and the3a*R*, 8a*S* diastereomer of okaramine H (**9**); and twelve previously reported analogues (**2**–**5**, **7**, **8**, and **10**–**15**) (Figure 1; refer to the Supporting Information for a detailed discussion of the structure characterization process for the new compounds).

To determine which of the secondary metabolites were responsible for the bioactive fraction's inhibitory properties, the purified compounds were tested individually over a 3 to

100 μM range in an XTT-based biofilm inhibition assay[32]. Two of the compounds, shearinines D (**3**) and E (**4**) (Figure 1), inhibit *C. albicans* DAY185 biofilm formation with IC_{50} values of 8.5 μM and 7.6 μM, respectively. The activities of **3** and **4** were also confirmed against a wild-type *C. albicans* SC5314, which is a virulent strain frequently used in animal infection studies and biofilm assays[33] (IC_{50} values of 2.68 μM and 1.99 μM, respectively). The XTT assay results for **3** were corroborated using confocal scanning laser microscopy. This revealed that *C. albicans* treated with 10 μM of **3** did not produce biofilms, but instead generated irregular, sparse layers in which the majority of cells lacked characteristic hyphal phenotypes (Figure 2, panels a and b). However, neither of the compounds appeared to inhibit the proliferation and viability of *C. albicans* at concentrations of up to 100 μM. Although we are limited in our ability to compare the structure-activity relationships of these compounds with only five shearinines available, it appears that a C-22 hydroxyl/methoxyl group is essential for bioactivity since the other shearinines lacking it were inactive at 30 SM (Figure 1).

Impact of Shearinine D on *C. albicans* Biofilms

Biofilms of *C. albicans* typically consist of complex consortia of cell types (*i.e.*, yeast, hyphae, pseudohyphae, and germ tube forms) embedded within extracellular matrices. Although substantial progress has been made to define the genetic and biological processes regulating the transition of *C. albicans* among these morphological states, there are significant gaps in this knowledge. The development of a quantitative, phenotypic screening tool could be expected to provide substantial insight concerning an inhibitor's mode of action by offering an effective method for analyzing the distribution of *C. albicans* morphological types following compound treatment.

Accordingly, we established a new imaging flow-cytometry technique, which enabled our group to discern the distribution of yeast, hyphae, pseudohyphae, and germ tube cells in *C. albicans* biofilms. Our method utilized an imaging flow cytometer (Amnis FlowSight®), which combined flow cytometry technology with fluorescent, darkfield, and brightfield cell imaging capabilities. The distinct advantage of using this approach was that it readily facilitated the assignment of biologically relevant gating parameters to complex cell mixtures since images of each recorded 'event' were available for inspection during post-experimental analysis. Although we had explored other (non-imaging-based) flow-cytometry approaches for characterizing biofilms (data not shown), none had proven satisfactory since the accurate delineation of phenotypically distinct cell populations could not be readily resolved without extensive sample pre-processing.

After seeding 96-well plates with *C. albicans* DAY185, cells were treated with compound **3** (10 and 50 SM), or vehicle only (DMSO). All experiments were performed in triplicate on two separate occasions. After enzymatically digesting the biofilm matrix, the samples were stained with propidium iodide (PI) and 10^4 events were analyzed by imaging flow-cytometry. The resulting image files were quantitatively analyzed and the compiled data were used to generate a two-dimensional plot displaying each event as a function of its relative aspect ratio (length:width) and size (area) (Figure 3, panel a). This yielded three distinct event populations (fields R4, R5, and R6) representing different types of cell morphologies. Field R4 was comprised of spherical cells with yeast-like morphologies, while field R5 was populated by elongated cells with germ tubes/hyphal buds (Figure 3, panel b). In contrast, field R6 consisted of an unresolved mixture of varyingly branched hyphae along with biofilm matrix and cell debris (*e.g.*, dead cells and cell fragments). Consequently, several hundred images files obtained for events in the R6 region were manually inspected to identify an operational set of gating parameters that enabled the further subdivision of this group. This resulted in the separation of the R6 region into two

subgroups based on each particle's maximal thickness and fluorescence contrast (Figure 3, panel a). The resulting R7 cluster contained cells with one or more hyphal branch points, while the R8 cluster consisted almost entirely of biofilm matrix and cell debris (Figure 3, panel b). Further analysis of the R7 region demonstrated that this cluster contained pseudohyphae that displayed significant "circularity" and true hyphae, which exhibited less circularity and more diffuse PI staining (*i.e.*, the stained nuclei of true hyphae are typically spread further apart along the length of the hyphal axis, whereas the nuclei of psuedohyphae are usually found in closer proximity to one another due to their irregular branching). This combination of features (*i.e.*, spot intensity minimum and circularity) enabled the separation of the R7 region into two groups, pseudohyphae (R9) and hyphae (R10).

Using this approach, it was revealed that the morphological state distribution of *C. albicans* cells administered **3** was substantially altered compared with vehicle-only-treated controls (Figure 3, panel c). Following exposure to **3**, the proportion of budding yeast cells (R4) was significantly increased, while the numbers of germ tube cells (R5), pseudohyphae (R9), and hyphae (R10) were significantly reduced. Taken together, these data indicate that compound **3** inhibits the hyphae formation process in *C. albicans*.

The process of *Candida* biofilm formation and maturation is rather complex encompassing four distinct stages involving cell adherence, hyphae formation, production of an extracellular matrix, and dispersal.[34,35] Consequently, *Candida* biofilms contain a diverse population of cell types that are essential to their function.[36] Considering the potential clinical value of targeting *Candida* biofilms, characterizing the activity spectrum for each new bioactive agent will play an important role in appraising their functional roles. To date, many methods for studying the morphological distribution of cells in *Candida* biofilms have been proposed.[37] Both microscopy[38] and traditional flow cytometry[39,40] have been used to analyze specific features of these cell populations such as the presence of germ tubes and hyphae. To the best of our knowledge, none of these methods are altogether capable of concurrently providing a quantitative assessment of the full range of cell types contained within *Candida* biofilms. Furthermore, it has been our experience that microcopy-based assay approaches require a substantial investment of time to manually score each sample. This new method promises a fast and precise approach to sample evaluation, which is crucial for conducting a robust natural-products- based (or other chemical source) screening program.

Shearinines Block Hyphae Formation

To further characterize the inhibitory activities of the shearinines, the effects of **3** and **4** were assessed against both nascent and intact biofilms. Both compounds substantially suppressed hyphal outgrowth in developing biofilms at concentrations of 30 μM (Figure 4, panel a), which led to an accumulation of metabolically active (based on XTT assay) pseudohyphae. These results were compared to the effects 5,8,11,14-eicosatetraynoic acid (ETYA), which had been reported to function as a yeast-to-hyphae transition inhibitor.[25] As expected, *C. albicans* biofilm formation was blocked in cells treated with the reference compound, whereas cell viability and proliferation persisted at concentrations as high as 100 μM. However, the resulting pseudohyphae exposed to as little as 30 μM ETYA exhibited marked cellular swelling, which was in contrast to the normal-looking pseudohyphae that resulted from administration of either shearinine (Figure 4, panel a).

The activities of **3** and **4** were assessed in a time-of-addition assay to determine when during the biofilm development process *C. albicans* was responsive to the inhibitory effects of the shearinines (Figure 4, panel b). Unlike waikialoid A, another potent biofilm inhibitor that was recently described by our group,[29] compounds **3** and **4** showed an extended spectrum of activity that resulted in relatively similar levels of biofilm-formation disruption at time

points of up to 6 h after *C. albicans* inoculation. This timeline of activity is consistent with the flow cytometry observations that shearinines have little effect on the relative proportion of *C. albicans* cells exhibiting germ tubes, but instead have a more striking effect on limiting the fraction of cells exhibiting extended and/or branched hyphae. These data support the conclusion that compounds **3** and **4** impact a stage in the biofilm development process that is activated much later than the target disrupted by waikialoid A.

The disruption of pre-formed biofilms is considered an important attribute for the development of a therapeutically useful agent capable of combating established *C. albicans* infections. In these cases, antibiotics such as amphotericin B and caspofungin exhibit reduced efficacy due to limited drug penetrance. This results in the need for dosing patients with much higher levels of the drugs, which poses significant toxicological risks.[41] Both **3** and **4** were able to cause the partial disruption and detachment of pre-formed *C. albicans* biofilm in a dose-dependent manner resulting in 51 ± 2 % and 34 ± 1 % reductions, respectively, of 48 h-old biofilm at 100 μM (Figure 4, panel c). Cells freed from the biofilms remained viable, which was consistent with our previous observation that the shearinines are not acutely toxic to *C. albicans*. Whereas an initial model rationalizing the higher concentrations of shearinines required for disrupting pre-formed biofilms could involve their limited permeation into the biofilm matrix, we find this explanation to be incongruous with other observations made in the course of our experiments. Namely, 10× reduced concentrations of shearinines were found to be efficacious at synergistically enhancing the antifungal activity of amphotericin B against established biofilms (*vida infra*). Therefore, it is likely that the activities of the shearinines against established biofilms involve a mechanism unrelated to the disruption of their formation.

Shearinines Synergize with Amphotericin B against *Candidas*.

The abilities of **3** and **4** to enhance the antifungal activity of the clinically-approved agent, amphotericin B, were also tested. This is important because biofilms are reported to increase the resistance of *Candida* to antifungal therapies.[42] Whereas the shearinines did not inhibit the viability or proliferation of *C. albicans* at concentrations of up to 100 μM, the addition of 2.5 μM or more of **3** and **4** to cells treated with a subtherapeutic dose (0.2 μM) of amphotericin B (MIC = 2.5 μM) substantially enhanced its potency against *C. albicans* in developing biofilms (Figure 5, panel a). Treatment of cells with 2.5 μM **3** or **4** resulted in an approximately eight-fold increase in the potency of amphotericin B (Figure 5, panel b). The presumed synergistic activities of compounds **3** and **4** were tested in a checkerboard assay,[43] which is used to delineate synergistic drug combinations. This analysis confirmed the proposed synergistic effects of **3** and **4** with both compounds affording FICI indices of < 0.12 (Table 1). The synergistic activities of **3** and **4** against *C. albicans* DAY185 grown on silicone discs were also observed by fluorescence microscopy (Figure 5, panel c). Initially, concentrations of **3** (5 SM) and amphotericin B (0.3 SM) were identified that were not able to inhibit *C. albicans* hyphae formation or cell proliferation, respectively. However, when **3** and amphotericin B were co-administered to *C. albicans* at these same concentrations, the combination treatment was effective at arresting cell growth. The same combination of the two agents showed a similar synergistic effect against another isolate, *C. albicans* SC5314 (Supplementary Table S2). The synergistic effects of shearinines and amphotericin B were also tested against established *C. albicans* biofilms. However, the combination treatment provided a more marginal enhancement of amphotericin B's antifungal activity (Figure 5, panel d).

In light of the synergistic effects exhibited by shearinines with amphotericin B against *C. albicans*, we investigated if similar antagonistic effects could be achieved against a wider selection of *Candida* spp. A total of 28 clinical isolates representing six *Candida* spp. were

obtained from the University of Oklahoma Medical Center (*C. albicans*: 11 isolates, *Candida glabrata*: 8 isolates, *Candida parapsilosis*: 6 isolates, *Candida tropicalis*: 1 isolate, *Candida kefyr*: 1 isolate, and *Candida krusei*: 1 isolate) and each specimen was evaluated in the checkerboard assay. We found that 16 of the strains exhibited synergistic responses to the combination treatment of amphotericin B and compound **3** (Table 2 and Supplementary Table S2). Cell proliferation was not inhibited by **3** in any of the isolates at concentrations of up to 100 μM. Interestingly, 10 of the Candida isolates were unable to form hyphae or pseudohyphae under the conditions tested in our lab (Supplementary Table S2); whereas, only four of these isolates failed to exhibit synergistic sensitivities to the combination of **3** and amphotericin B. These data imply that the shearinines might (*a*) act through a mechanism that impacts a more global cellular process that affects pathways beyond those solely involved in hyphae formation and biofilm formation or (*b*) disrupt multiple biological targets.

Summary and Future Directions

In light of the deleterious effects that *C. albicans* and other *Candida* spp. have on human health, new strategies must be implemented to combat these infectious pathogens. Targeting *Candida* biofilms has been identified as one such approach.[9] However, concerns over the spectrum of protection afforded by this tactic, as well as the potential to reliably enhance the efficacy of existing antifungal therapeutics has tempered the biomedical community's willingness to enthusiastically embrace this methodology. This study offers support for the concept that small-molecules which targeted biofilm-related processes are potentially useful tools for improving clinicians' abilities to exert pharmacological control over *Candida* infections. The synergistic effects of the shearinines present a promising opportunity for exploring how the currently limited range of antifungal antibiotic options could be strengthened to more effectively combat *Candida* infections. Moreover, the synergistic activities of the shearinines point to a potentially useful strategy for helping to limit the significant toxic side effects associated with amphotericin B use. By lowering the amount of amphotericin B that is administered to patients, there is the potential to alleviate many of the drug's self-limiting properties such as nausea and vomiting, fever, breathing difficulties, and nephrotoxicity.[44] The shearinines are a good tool for testing the potential advantages of using adjunctive therapies in combination with antifungals. Despite these intriguing activities, further research will be needed to determine whether the biofilm disruption effects and synergism with amphotericin B are related through a single cellular target or result from the disruption of multiple targets. Nevertheless, given the wide spectrum of unique *Candida* biofilm disrupting compounds that have been detected from our initial natural products studies,[29–31] we are optimistic that new and more potent bioactive compounds will emerge as prospective candidates for preclinical exploration.

METHODS

Strains and Medium

The reference strain *C. albicans* DAY185[45] was the gift from C. A. Kumamoto (Tufts University) and A. Mitchell (Carnegie Mellon University), and *C. albicans* SC5314[33] was the gift from A. Dongari-Bagtzoglou (University of Connecticut Health Center). Clinical isolates were obtained from the University of Oklahoma Medical Center (*C. albicans*: 11 isolates, *Candida glabrata*: 8 isolates, *Candida parapsilosis*: 6 isolates, *Candida tropicalis*: 1 isolate, *Candida kefyr*: 1 isolate, and *Candida krusei*: 1 isolate). These strains were cultured in brain heart infusion medium (BHI medium, Becton Dickinson) or RPMI-1640 plus MOPS medium [RPMI-1640 medium (Sigma) buffered to pH 7.0 with 0.17 M MOPS (3-(Nmorpholino) propanesulfonic acid, Sigma)] as required.

Assays for Growth Inhibition and Biofilm Formation

The effects of compounds on the growth of *C. albicans* were tested using the method described in the NCCLS 2002 CLSI M27- A2 guidelines.[29] The biofilm assay was performed as described with the following modifications. Cells of *C. albicans* DAY185 or SC5314 were cultured in BHI medium (Becton Dickinson) at 37 °C overnight. The cells were pelleted by centrifugation, washed with sterile PBS (phosphate-buffered saline, pH 7.4), and resuspended in RPMI-1640 plus MOPS medium. Test compounds were prepared in DMSO at stock concentrations of 20 mM before being serially diluted in RPMI-1640 plus MOPS medium for testing. 5,8,11,14-Eicosatetraynoic acid (ETYA, Santa Cruz Biotechnology) was used as a positive control. Aliquots of yeast suspension (100 μL containing 2.5×10^3 cells mL^{-1}) were added to the medium containing the diluted compounds or DMSO [final concentrations did not exceed 1% (v/v)] before being transferred to 96-well plates (Corning). After 48 h of incubation at 37 °C, the viability of the yeast was measured using the XTT assay.[32] In brief, yeast cells were treated with 0.1 mg mL^{-1} XTT at 37 °C for 1 h. Absorbance measurements were taken at 492 nm using a microplate reader (Infinite M200). The minimum inhibitory concentrations (MIC) for growth were defined as the lowest antifungal concentrations that caused ≥85% reduction in metabolic activity.

For measuring biofilm formation, the medium was aspirated and the wells were washed twice with sterile PBS to remove non-adherent cells. Fresh medium (100 SL RPMI-1640 plus MOPS) was then added back to each well. The formation of biofilms was measured using the XTT assay. All experiments were performed in triplicate on three separate occasions. The 50% inhibitory concentration values (IC_{50}) for biofilm inhibition were calculated using GraphPad Prism 5.

Biofilm Formation on Silicone Discs

Biofilms were formed on silicone discs (Bentec Medical).[37] In brief, silicone elastomer discs were pretreated with fetal bovine serum and inoculated with *C. albicans* DAY185, which were recovered in BHI medium and washed with sterile PBS. After incubating at 60 rpm agitation at 37 °C for 90 min, the silicone discs were washed with sterile PBS to remove adhered cells and transferred to 6-well plates with 3 mL RPMI-1640 plus MOPS medium. After adding DMSO (vehicle control), amphotericin B, test compound, or amphotericin B plus test compound, the plates were incubated on a shaker incubator (60 rpm agitation at 37 °C for 48 h). The silicone discs were stained with Alexa Fluor 488 conjugated concanavalin A (Invitrogen) in the dark at 37 °C for 30 min and biofilms observed by confocal laser scanning microscopy (Leica) or fluorescence microscope (Molecular Devices).

Morphological Analysis by Imaging Flow Cytometry

Cells of *C. albicans* DAY185 were seeded in 96-well plates at 5×10^4 cells $well^{-1}$ and treated with DMSO or test compound in RPMI-1640 plus MOPS medium at 37 °C for 24 h. After discarding the medium, the bioflims were digested with lyticase (Sigma) at 37 °C for 30 min.[46] The digested cells were washed with 1 M sorbitol (Sigma) and fixed with 70% ethanol/30% sorbitol[47] at 4 °C for 36 h. After washing with PBS, the cells were treated with ribonuclease A (Amresco) and stained by propidium iodide (PI; Sigma) at 37 °C for 30 min.[48] The cell suspensions were analyzed using an ImageStream imaging flow cytometer (Amnis Corporation).

Hyphae Formation Assay.[29]

Cells of *C. albicans* was grown in BHI medium at 37 °C overnight. The cells were pelleted, washed, and suspended in sterile PBS (pH 7.4). Cells were seeded in 96-well plates at 1×10^6

cells well^{-1} and incubated at 37 °C for 1 h. Wells were washed twice with sterile PBS to remove non-adherent cells. RPMI-1640 containing 2% (w/v) glucose and compound in DMSO [final concentration did not exceed 1% (v/v)] were added to each well and the plates were incubated at 37 °C for 24 h. Hyphae formation was observed with a phase contrast microscope.

Biofilm Time-of-Addition Assay

Using the techniques described above for the biofilm formation inhibition assay, compounds (from 3 to 100 μM) were added at 0, 2, 4, 6, 8, 12 h after seeding *C. albicans* DAY185 cells in a 96-well microplate. At 48 h after inoculation, the wells were washed twice with PBS and the amount of cells and biofilm were determined by XTT assay. The IC_{50} values for biofilm reduction were calculated using GraphPad Prism 5. All experiments were performed in triplicate on three separate occasions.

Pre-Formed Biofilm Assay

The methods used to assess established biofilms were the same as those described above except that *C. albicans* DAY185 cells were cultured in RPMI-1640 plus MOPS medium in a 96-well microplate at 37 °C for 24 h ("24 h-old biofilm") or 48 h ("48 h-old biofilm") prior to treatment with test compounds.

Checkerboard Assay for Synergistic Effects

To evaluate the synergistic effects of shearinines and amphotericin B, a checkerboard assay was used.[43] *Candida* cells were seeded in 96-well plates and treated with different concentration of test compounds and amphotericin B, alone or in combination in RPMI-1640 plus MOPS medium at 37 °C for 48 h. The viability of the yeast was measured using the XTT assay and the MIC for growth was defined as the lowest antifungal concentrations that caused ≥85% reduction in the metabolic activity. The interactions of test compounds and amphotericin B were based on the fractional inhibitory concentration index (FICI).[43] FICI values are calculated as follows: $(MIC_{Drug\ A\ in\ combination}/MIC_{Drug\ A\ alone})+(MIC_{Drug\ B\ in\ combination}/MIC_{Drug\ B\ alone})$. The interpretation of the FICI is determined as follows: ≤ 0.5, synergistic effect; > 0.5 but < 4, indifference; and ≥ 4, antagonistic effect.

Statistical Analysis

Results were expressed as the means ± standard deviations. Analyses were performed using two-tail Student's *t*-tests. *P* values < 0.05 were considered statistically significant.

Supplementary Material

Refer to Web version on PubMed Central for supplementary material.

Acknowledgments

We thank C. Kumamoto (Tufts University, USA) and A. Mitchell (Carnegie Mellon University, USA) for the supplying the *C. albicans* DAY185 strain and A. Dongari-Bagtzoglou (University of Connecticut Health Center, USA) for the supplying the *C. albicans* SC5314 strain. We appreciate help from G. Griffith for providing the soil sample from which KS-017 was obtained. Research reported in this publication was supported by the National Institute of Allergy and Infectious Diseases of the National Institutes of Health under award number RO1AI085161. The content is solely the responsibility of the authors and does not necessarily represent the official views of the National Institutes of Health.

References

1. Lass-Florl C. The changing face of epidemiology of invasive fungal disease in Europe. Mycoses. 2009; 52:197–205. [PubMed: 19391253]
2. Ruan SY, Hsueh PR. Invasive candidiasis: an overview from Taiwan. J Formos Med Assoc. 2009; 108:443–451. [PubMed: 19515624]
3. Playford EG, Nimmo GR, Tilse M, Sorrell TC. Increasing incidence of candidaemia: long-term epidemiological trends, Queensland, Australia, 1999–2008. J Hosp Infect. 2010; 76:46–51. [PubMed: 20382444]
4. Falagas ME, Roussos N, Vardakas KZ. Relative frequency of albicans and the various non-albicans *Candida* spp. among candidemia isolates from inpatients in various parts of the world: a systematic review. Int J Infect Dis. 2010; 14:e954–e966. [PubMed: 20797887]
5. Hobson RP. The global epidemiology of invasive *Candida* infections – is the tide turning? J Hosp Infect. 2003; 55:159–168. [PubMed: 14572481]
6. Pfaller MA, Diekema DJ. Epidemiology of invasive candidiasis: a persistent public health problem. Clin Microbiol Rev. 2007; 20:133–163. [PubMed: 17223626]
7. Tumbarello M, Fiori B, Trecarichi EM, Posteraro P, Losito AR, De Luca A, Sanguinetti M, Fadda G, Cauda R, Posteraro B. Risk factors and outcomes of candidemia caused by biofilm-forming isolates in a tertiary care hospital. PLoS ONE. 2012; 7:e33705. [PubMed: 22479431]
8. Tumbarello M, Posteraro B, Trecarichi EM, Fiori B, Rossi M, Porta R, de Gaetano Donati K, La Sorda M, Spanu T, Fadda G, Cauda R, Sanguinetti M. Biofilm production by *Candida* species and inadequate antifungal therapy as predictors of mortality for patients with candidemia. J Clin Microbiol. 2007; 45:1843–1850. [PubMed: 17460052]
9. Harriott MM, Noverr MC. Importance of *Candida*–bacterial polymicrobial biofilms in disease. Trends Microbiol. 2011; 19:557–563. [PubMed: 21855346]
10. Harriott MM, Lilly EA, Rodriguez TE, Fidel PL, Noverr MC. *Candida albicans* forms biofilms on the vaginal mucosa. Microbiology. 2010; 156:3635–3644. [PubMed: 20705667]
11. Ganguly S, Mitchell AP. Mucosal biofilms of *Candida albicans*. Curr Opin Microbiol. 2011; 14:380–385. [PubMed: 21741878]
12. Douglas LJ. *Candida* biofilms and their role in infection. Trends Microbiol. 2003; 11:30–36. [PubMed: 12526852]
13. Nett JE, Sanchez H, Cain MT, Andes DR. Genetic basis of *Candida* biofilm resistance due to drug-sequestering matrix glucan. J Infect Dis. 2010; 202:171–175. [PubMed: 20497051]
14. Nett JE, Sanchez H, Cain MT, Ross KM, Andes DR. Interface of *Candida albicans* biofilm matrix-associated drug resistance and cell wall integrity regulation. Eukaryot Cell. 2011; 10:1660–1669. [PubMed: 21666076]
15. Lewis K. Persister cells. Annu Rev Microbiol. 2010; 64:357–372. [PubMed: 20528688]
16. Dawson CC, Intapa C, Jabra-Rizk MA. “Persisters”: survival at the cellular level. PLoS Pathog. 2011; 7:e1002121. [PubMed: 21829345]
17. LaFleur MD, Qi Q, Lewis K. Patients with long-term oral carriage harbor high-persister mutants of *Candida albicans*. Antimicrob Agents Chemother. 2010; 54:39–44. [PubMed: 19841146]
18. LaFleur MD, Kumamoto CA, Lewis K. *Candida albicans* biofilms produce antifungal-tolerant persister cells. Antimicrob Agents Chemother. 2006; 50:3839–3846. [PubMed: 16923951]
19. Ramage G, Martinez JP, Lopez-Ribot JL. *Candida* biofilms on implanted biomaterials: a clinically significant problem. FEMS Yeast Res. 2006; 6:979–986. [PubMed: 17042747]
20. Hasan F, Xess I, Wang X, Jain N, Fries BC. Biofilm formation in clinical *Candida* isolates and its association with virulence. Microbes Infect. 2009; 11:753–761. [PubMed: 19409507]
21. Kojic EM, Darouiche RO. *Candida* infections of medical devices. Clin Microbiol Rev. 2004; 17:255–267. [PubMed: 15084500]
22. Chandra J, Mukherjee P, Ghannoum M. Fungal biofilms in the clinical lab setting. Current Fungal Infection Reports. 2010; 4:137–144.

23. Toenjes KA, Stark BC, Brooks KM, Johnson DI. Inhibitors of cellular signalling are cytotoxic or block the budded-to-hyphal transition in the pathogenic yeast *Candida albicans*. J Med Microbiol. 2009; 58:779–790. [PubMed: 19429755]
24. Midkiff J, Borochoff-Porte N, White D, Johnson DI. Small molecule inhibitors of the *Candida albicans* budded-to-hyphal transition act through multiple signaling pathways. PLoS ONE. 2011; 6:e25395. [PubMed: 21966518]
25. Grald A, Yargosz P, Case S, Shea K, Johnson DI. Small-molecule inhibitors of biofilm formation in laboratory and clinical isolates of *Candida albicans*. J Med Microbiol. 2012; 61:109–114. [PubMed: 21903824]
26. Shareck J, Belhumeur P. Modulation of morphogenesis in *Candida albicans* by various small molecules. Eukaryot Cell. 2011; 10:1004–1012. [PubMed: 21642508]
27. Newman DJ, Cragg GM. Natural products as sources of new drugs over the 30 years from 1981 to 2010. J Nat Prod. 2012; 75:311–335. [PubMed: 22316239]
28. Newman DJ, Cragg GM. Natural products as sources of new drugs over the last 25 years. J Nat Prod. 2007; 70:461–477. [PubMed: 17309302]
29. Wang X, You J, King JB, Powell DR, Cichewicz RH. Waikialoid A suppresses hyphal morphogenesis and inhibits biofilm development in pathogenic *Candida albicans*. J Nat Prod. 2012; 75:707–715. [PubMed: 22400916]
30. Wang X, Du L, You J, King JB, Cichewicz RH. Fungal biofilm inhibitors from a human oral microbiome-derived bacterium. Org Biomol Chem. 2012; 10:2044– 2050. [PubMed: 22281750]
31. Gerea AL, Branscum KM, King JB, You J, Powell DR, Miller AN, Spear JR, Cichewicz RH. Secondary metabolites produced by fungi derived from a microbial mat encountered in an iron-rich natural spring. Tetrahedron Lett. 2012; 53:4202–4205. [PubMed: 22844162]
32. Nett JE, Cain MT, Crawford K, Andes DR. Optimizing a *Candida* biofilm microtiter plate model for measurement of antifungal susceptibility by tetrazolium salt assay. J Clin Microbiol. 2011; 49:1426–1433. [PubMed: 21227984]
33. Ramage G, Saville SP, Wickes BL, Lopez-Ribot JL. Inhibition of *Candida albicans* biofilm formation by farnesol, a quorum-sensing molecule. Appl Environ Microbiol. 2002; 68:5459–5463. [PubMed: 12406738]
34. Finkel JS, Mitchell AP. Genetic control of *Candida albicans* biofilm development. Nat Rev Micro. 2011; 9:109–118.
35. Uppuluri P, Chaturvedi AK, Srinivasan A, Banerjee M, Ramasubramaniam AK, Kohler JR, Kadosh D, Lopez-Ribot JL. Dispersion as an important step in the *Candida albicans* biofilm developmental cycle. PLoS Pathog. 2010; 6:e1000828. [PubMed: 20360962]
36. Sardi JC, Scorzoni L, Bernardi T, Fusco-Almeida AM, Mendes Giannini MJ. *Candida* species: current epidemiology, pathogenicity, biofilm formation, natural antifungal products and new therapeutic options. J Med Microbiol. 2013; 62:10–24. [PubMed: 23180477]
37. Chandra J, Mukherjee PK, Ghannoum MA. In vitro growth and analysis of *Candida* biofilms. Nat Protoc. 2008; 3:1909–1924. [PubMed: 19180075]
38. Decanis N, Tazi N, Correia A, Vilanova M, Rouabhia M. Farnesol, a fungal quorum-sensing molecule triggers *Candida albicans* morphological changes by downregulating the expression of different secreted aspartyl proteinase genes. Open Microbiol J. 2011; 5:119–126. [PubMed: 22207890]
39. Barelle CJ, Bohula EA, Kron SJ, Wessels D, Soll DR, Schafer A, Brown AJ, Gow NA. Asynchronous cell cycle and asymmetric vacuolar inheritance in true hyphae of *Candida albicans*. Eukaryot Cell. 2003; 2:398–410. [PubMed: 12796285]
40. Calvert MEK, Lannigan JA, Pemberton LF. Optimization of yeast cell cycle analysis and morphological characterization by multispectral imaging flow cytometry. Cytom Part A. 2008; 73:825–833.
41. Ramage G, VandeWalle K, Bachmann SP, Wickes BL, Lopez-Ribot JL. In vitro pharmacodynamic properties of three antifungal agents against preformed *Candida albicans* biofilms determined by time-kill studies. Antimicrob Agents Chemothe. 2002; 46:3634–3636.
42. Mukherjee PK, Chandra J. *Candida biofilm* resistance. Drug Resist Update. 2004; 7:301–309.

43. Vitale RG, Afeltra J, Dannaoui E. Antifungal combinations. Methods Mol Med. 2005; 118:143–152. [PubMed: 15888940]
44. Laniado-Laborin R, Cabrales-Vargas MN. Amphotericin B: side effects and toxicity. Rev Iberoam Micol. 2009; 26:223–227. [PubMed: 19836985]
45. Breger J, Fuchs BB, Aperis G, Moy TI, Ausubel FM, Mylonakis E. Antifungal chemical compounds identified using a *C. elegans* pathogenicity assay. PLoS Pathog. 2007; 3:168–178.
46. Al-Fattani MA, Douglas LJ. Biofilm matrix of *Candida albicans* and *Candida tropicalis*: chemical composition and role in drug resistance. J Med Microbiol. 2006; 55:999–1008. [PubMed: 16849719]
47. Calvert ME, Lannigan JA, Pemberton LF. Optimization of yeast cell cycle analysis and morphological characterization by multispectral imaging flow cytometry. Cytom Part A. 2008; 73:825–833.
48. Ocampo A, Barrientos A. Quick and reliable assessment of chronological life span in yeast cell populations by flow cytometry. Mech Ageing Dev. 2011; 132:315–323. [PubMed: 21736893]

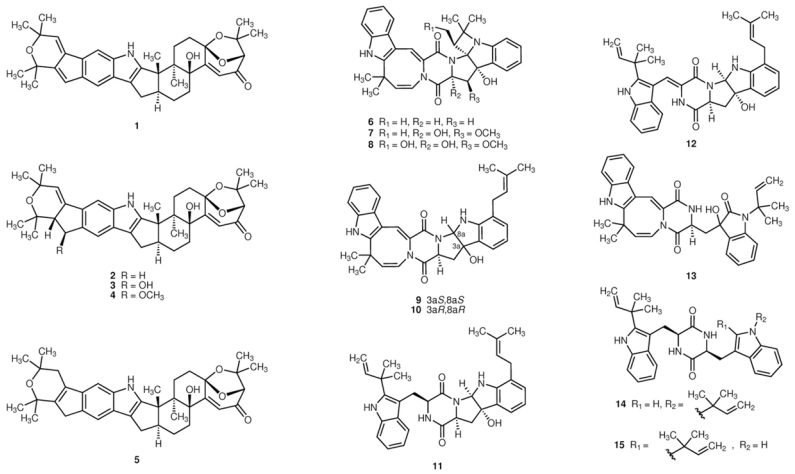

Figure 1.

Structures of alkaloid metabolites produced by an Alaskan-soil-derived *Penicillium* sp. The purified compounds 22,23-dehydro-shearinine A (**1**) and shearinines A (**2**), D (**3**), E (**4**), and F (**5**); 2-dehydroxy-3-demethoxy-okaramine B (**6**) and the 3a*R*, 8a*S* diastereomer of okaramine H (**9**); and twelve previously reported analogues (**2**–**5**, **7**, **8**, and **10**–**15**) were part of a complex of metabolites present in the bioactive (inhibition of *C. albicans* biofilm formation) fraction. Details of the isolation and structure determination of these compounds are provided in Supplementary Figure S1 and Table S1.

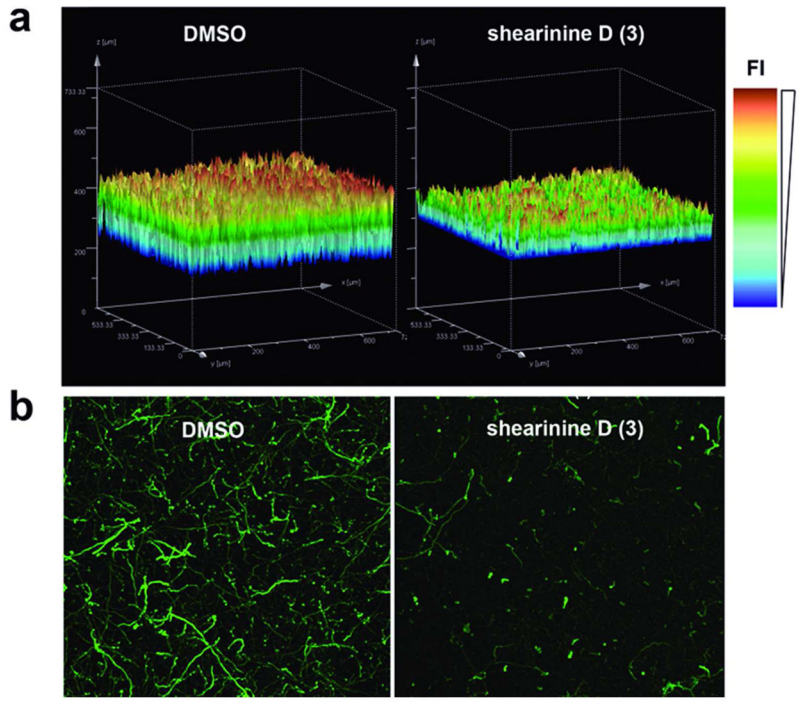

Figure 2.

Three-dimensional confocal laser scanning microscopy images of *C. albicans* biofilms treated with DMSO or 10 μM shearinine D (**3**). **a)** The top panel provides a reconstructed image detailing the thickness and fluorescence intensity of treated and untreated biofilms (note that the colors represent varying fluorescent intensity (FI) throughout the biofilm). **b)** A compilation of *Z*-stack photos taken of the biofilm surface reveals a large number of long hyphae in the control group forming an interwoven network of cells; whereas, samples treated with compound **3** exhibit very few hyphae and cells that did not assemble into a biofilms. All experiments were performed in triplicate on three separate occasions.

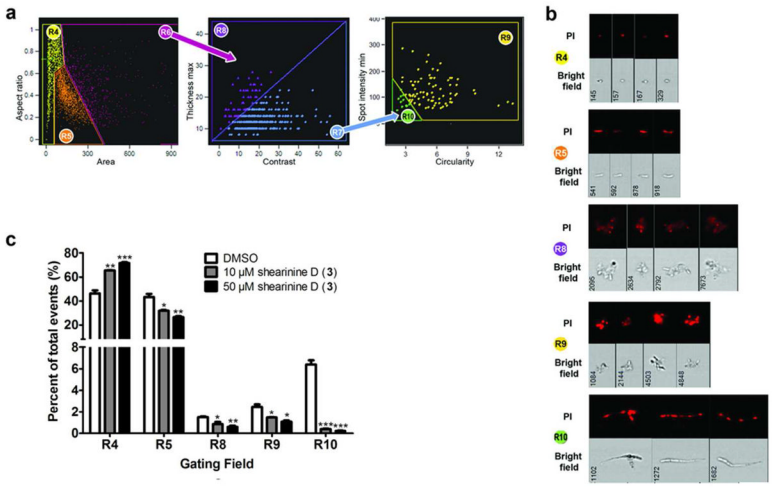

Figure 3.

The morphological distribution pattern of *C. albicans* cell types as revealed by imaging flow-cytometry. **a)** Distribution pattern of *C. albicans* cells and the gating parameters (R4–R10) that were used to demarcate each population. **b)** Images of cells representing each of defined populations: R4 (spherical cells with yeast-like morphologies), R5 (elongated cells with germ tubes/hyphal buds), R8 (biofilm matrix with cell debris), R9 (pseudohyphae), and R10 (hyphae). **c)** The graph showed the population distributions for each cell type. Bars labeled with asterisks were determined to be statistically different from DMSO controls (*$P < 0.05$, **$P < 0.005$, ***$P < 0.001$). Data represent the mean values obtained from triplicate experiments on two separate occasions ± standard deviations.

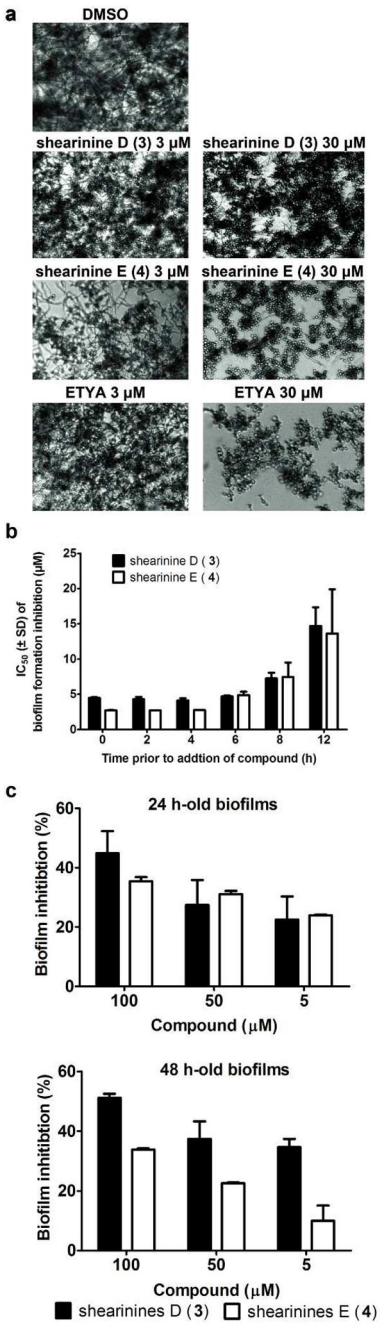

Figure 4.

The effect of shearinines D (**3**) and E (**4**) on *C. albicans* DAY185 biofilm formation. **a)** Both compounds **3** and **4** strongly inhibited hyphae formation at 30 μM, but only compound **4** exhibited activity at 3 μM. 5,8,11,14-Eicosatetraynoic acid (ETYA) was used as positive control. **b)** Time of addition assay showing that compounds **3** and **4** are still both effective at limiting biofilm formation for up to 6 h, which is well after germ tube formation and hyphae formation is initiated under these experimental conditions. **c)** Dose-response data revealing that **3** and **4** cause the detachment of pre-formed biofilms. Data represent the means of triplicate experiments performed on two separate occasions ± standard deviations.

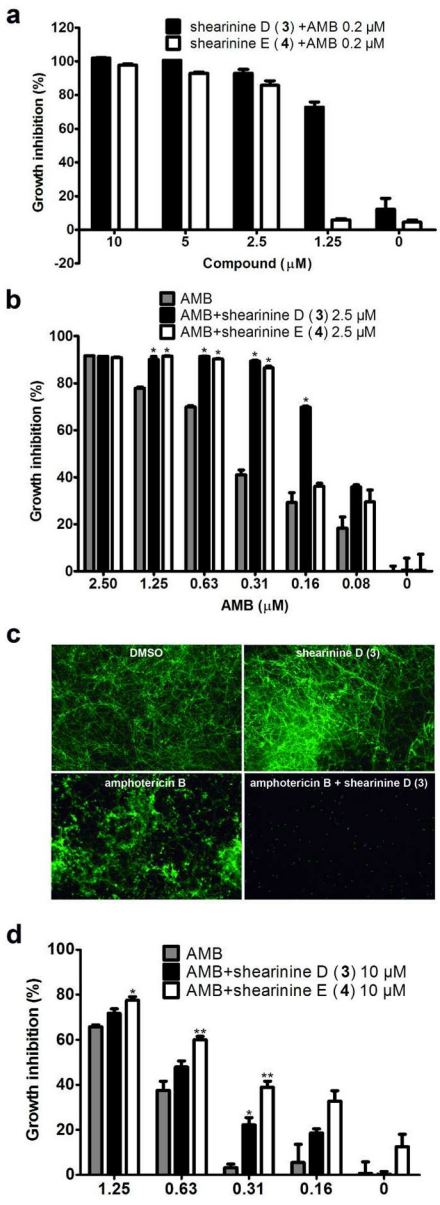

Figure 5.

Synergistic activities of shearinines D (**3**) and E (**4**) with amphotericin B (AMB) against *C. albicans*. **a)** The effects of 0.2 SM amphotericin B with different concentrations of compounds **3** and **4** on *C. albicans* growth. **b)** The effects of 2.5 SM of compounds **3** and **4** with different concentrations of amphotericin B on *C. albicans* growth. Sets of asterisks represents that results for cells administered the combination treatment were statistically different from amphotericin B-only-treated controls ($P < 0.05$). **c)** Fluorescence images of *C. albicans* treated with 5 SM **3** and 0.3 SM amphotericin B. **d)** Both **3** and **4** enhance the activity of amphotericin B against the 48 h-old *C. albicans* biofilms. Bars labeled with asterisks were determined to be statistically different from amphotericin B-treated controls (*$P < 0.05$, **$P < 0.01$). All experiments were performed in triplicate on three separate occasions.

Table 1

Summary of the synergistic interactions of amphotericin B (AMB) with shearinines D (3) and E (4) against *C. albicans* as determined by the checkerboard assay.[a]

Compound	AMB (μM)			Compound (μM)			FICI
	MIC_{single}[b]	$MIC_{combination}$	FIC	MIC_{single}	$MIC_{combination}$	FIC	
shearinine D **(3)**	2.5	0.12	0.25	> 100	2.5	< 0.025	< 0.12 S[c]
shearinine E **(4)**	2.5	0.12	0.25	> 100	2.5	< 0.025	< 0.12 S

[a] All experiments were performed in triplicate on three separate occasions.

[b] The MIC was defined as the lowest concentration causing ≥ 85% reduction in metabolic activity.

[c] Synergistic effect.

Table 2

Summary of the effects of amphotericin B and shearinine D (3) combinations against a panel of 28 *candida* clinical isolates.

Species	Number of isolates tested	Number of isolates exhibiting the indicated interaction		
		Synergistic effect	Indifference	Antagonistic effect
C. albicans	11	7	4	0
C. glabrata	8	5	3	0
C. parapsilosis	6	2	4	0
C. tropicalis	1	1	0	0
C. kefyr	1	1	0	0
C. krusei	1	0	1	0

All experiments were performed in triplicate on three separate occasions.